Contents lists available at ScienceDirect

Environmental Technology & Innovation

Photocatalytic NO$_x$ abatement: The effect of high air flow velocity

Eliska Mikyskova [a,*], Ivana Martiniakova [a,b], Radek Zouzelka [a,b], Jiri Rathousky [a,*]

[a] Center for Innovations in the Field of Nanomaterials and Nanotechnologies, J. Heyrovsky Institute of Physical Chemistry, Academy of Sciences of the Czech Republic, Dolejskova 3, Prague 18223, Czech Republic
[b] Advanced Materials – JTJ s.r.o., Kamenne Zehrovice 23, Kamenne Zehrovice 273 01, Czech Republic

ARTICLE INFO

ABSTRACT

In the literature, the abatement of nitrogen oxide (NO$_x$) emissions by photocatalysis is rarely carried out at real-world air flow velocities. Here, we investigated the performance of two commercial photocatalysts, Aeroxide$^{®}$ TiO$_2$ P25 (Evonik Industries, Germany) and FN NANO$^{®}$ 2 (Advanced Materials-JTJ, Czech Republic), P25 containing 88 % anatase and 12 % rutile, while FN 2 moreover 13 % of a binder. The degradation of NOx pollutants (0.1 and 1.0 ppmv) at air flow velocities ranging from 0.02 to 0.7 m s^{-1} was tested, the photocatalytic efficiency being determined for various slit heights (5–25 mm) and rate of volume flow (1500–11 000 cm^3 min^{-1}). The photocatalysts achieved substantial NO and NO$_2$ abatement. Pollutant conversion decreased as the air flow velocity increased, with the highest conversion (80%) occurring at 0.1 m s^{-1}. The NO$_x$ conversions were slightly higher for NO than for NO$_2$, and significantly higher for the NO concentration of 0.1 ppmv. Slit height had a negligible effect, indicating a substantial degree of mixing in the direction perpendicular to the flow; consequently, the flow cannot be laminar in nature as the ISO standard (22197-1:2016) states. This finding is supported by the nanoindentation technique showing that the surface roughness contributed to the formation of vortexes and enhancement of the mass transport. To our best knowledge, this is the first study to test commercial photocatalysts under such a wide range of air velocities and, in doing so, it has identified considerable implications for outdoor air purification.

1. Introduction

Reduction of air pollution is one of the most important environmental issues in recent decades worldwide. Nitrogen oxides (NO$_x$ = NO + NO$_2$) are considered as one of the most hazardous pollutant due to their toxicity on human health. Guerreiro et al. (2014) and Boyjoo et al. (2017) summarized the concentration limits recommended by many authorities, such as WHO or the U.S. Environmental Protection Agency. Therefore, it is crucial to keep their concentration on the long-term low levels.

Basically, there are two approaches how to achieve the NO$_x$ concentration decrease. Either to remove them at the place where they are formed, such as in the chimneys of factories or the exhaust of the cars (i). This process has the advantage of a relatively high pollutant concentration and the possibility to use higher pressure or temperature and the

---

* Corresponding authors.
E-mail addresses: eliska.mikyskova@jh-inst.cas.cz (E. Mikyskova), jiri.rathousky@jh-inst.cas.cz (J. Rathousky).

addition of supplementary reactants in the process of the pollutant degradation. Orto remove the pollutants dissipated in huge volumes of air (ii). The latter possibility is more demanding, however, very often the only one solution (Boyjoo et al., 2017; Cordero et al., 2020; Talaiekhozani et al., 2021).

Among advanced oxidation processes, which are a convenient choice for the degradation of pollutants, heterogeneous photocatalysis is often the only viable route. With regards of the applicability of this technology, several aspects are of major importance. First, a suitable photocatalytic coating with sufficient photocatalytic efficiency and durability is needed. With this aim in view, systems based on TiO_2 nanoparticles and stable binders have proven to be suitable. Second, a suitable methodology using which will enable to realistically determine the performance of photocatalytic coatings at expected environmental conditions is missing.

Further, with respect to laboratory experiments, the effect of relevant process parameters on the efficiency of the photocatalytic technology should be determined. In principle, there are four types of these parameters, namely the irradiation, air humidity, the composition of the gaseous mixture and the character of air flow. The effect of the irradiation intensity wavelength has been dealt with in a number of published studies (Devahasdin et al., 2003; Ballari et al., 2010, 2011; Dillert et al., 2012; Binas et al., 2017). Regarding the composition, quite a lot of studies focused on a single pollutant (such as NO_x or VOC) taking into an account the variation in the air relative humidity (e.g., Ao and Lee, 2003; Vogel et al., 2003; Wang et al., 2007; Chen and Chu, 2011; de O.B. Lira et al., 2019). However, with respect to mixtures of several pollutants, the literature is much scarcer.

Finally, the effect of the character of air flow on the photocatalytic performance was addressed mostly marginally, as a supplement to the research devoted to other topics. Up to now, the papers published revealed considerable uncertainties in the flow regime description related to the relatively narrow range of flow parameters, especially the volume rate of flow, velocity or the cross-sectional area. For instance, Demeestere et al. (2004) characterized gas flow patterns in the photoreactor using the gas residence time distribution curves. They concluded the degree of axial dispersion was low, which should indicate a turbulent flow regime, even at the lowest volume rate of flow (Demeestere et al., 2004). On the other hand, Tomašić et al. (2008) described the flow regime in their reactor as a plug flow in the axial direction with molecular diffusion transfer in the radial direction. Even sophisticated computational fluid dynamic models show often different results strongly depending on the input parameters (Castrillón and De Lasa, 2007; Imoberdorf et al., 2007; Queffeulou et al., 2010; Muñoz et al., 2019).

Generally, in the published studies, the velocities of the flowing air are lower than typically encountered at real conditions. Consequently, the space (or residence) times are longer, which influences the observed performance and the reliability of the extrapolation of the laboratory data to the real-world conditions.

Our study is focused on commercial photocatalysts, which are composed primarily of TiO_2 due to the advantages of this material, e.g. suitable photocatalytic activity, is applicable to a wide range of pollutants, proves high photocatalytic stability and sufficient absorption in the UV-A field. An important parameter is also its non-toxicity, eco-friendly and price (Park et al., 2013; Guo et al., 2019)

Therefore, the present study is aimed at the systematic experimental research into the effect of air flow through the photoreactor at a wide range of conditions, which enables to model realistic situations encountered in the real application of photocatalytic technology for the purification of air. The extensive experimental data obtained will contribute for the photocatalytic technology to stop being only 'promising' and to become a true applicable and sustainable technology. In our study, we included higher velocities of the flowing air which are close to realistic values encountered in real exterior applications. We tested a commercially produced functional paint with very good mechanical properties and excellent adhesion to the substrate.

2. Materials and methods

2.1. Preparation and characterization of photocatalytic layers

In this study, two types of TiO_2-based photocatalysts were tested. Evonik Aeroxide P25 (referred as P25) was chosen as a standard material, because of its high photocatalytic activity, large surface area, low cost and easy availability. It possesses a relatively well-defined composition, consisting mainly of rutile and anatase in the ratio of 80:20 with some small proportion of amorphous titania.

As the research performed is aimed at the real application of photocatalysis for the purification of air, the industrially produced photocatalytic material FN$^{®}$2 NANO coating (here referred as FN2) was selected, which is produced by the Advanced Materials-JTJ company (Czech Republic) and is protected by U.S. patent no. 8,647,565 (2009). FN2 consists mainly of about 74% of Aeroxide TiO_2 P25, the remaining part being an inorganic binder.

The given photocatalysts were mixed with deionized water to form an 8 wt. % suspension. To ensure the homogeneous distribution on the substrate, the suspension was coated onto glass plates $5 \times 10 \times 0.5$ cm in size using an airbrush spray gun (Knightsbridge PME$^{®}$ Ltd., Enfield, UK, SFig. 1). The glass substrate was preheated before application. The application took place in several layers to final sample weight of 50 mg. Prepared photocatalytic layers were placed into an exicator, to avoid the contact with laboratory environment.

Phase and crystallinity analysis was performed with PANalytical diffractometer X'Pert Pro equipped with a Co$K\alpha_1$ tube ($\lambda = 0.178901$ nm) in the Bragg–Brentano arrangement. The diffraction patterns were evaluated by the Rietveld method

using the TOPAS 3 software (Bruker AXS GmbH, Karlsruhe, Germany). The specific surface area (S_{BET}) of the coatings was determined by an analysis of adsorption isotherms of N_2 at 77 K performed with a Micrometrics 3Flex (Micromeritics Instrument Corporation, Norcross, GA, USA) adsorption unit. The structure of the photocatalytic layers was determined with Jeol JEM-2100 UHR transmission microscope and Jeol JSM-5500LV (both JEOL Ltd., Tokyo, Japan) scanning electron microscope. The optical properties of the layers were measured with a PerkinElmer Lambda 950 UV–Vis–NIR spectrometer equipped with Spectralon (PerkinElmer Inc., Waltham, MA, USA). The physico-chemical properties of P25 and FN2 coatings were detailly discussed by Zouzelka and Rathousky (2017). The topography of photocatalytic was measured performing by Hysitron TI980 Nanoindenter (Bruker AXS GmbH, Karlsruhe, Germany).

2.2. Photocatalytic experimental set-up

The determination of the photocatalytic performance of photocatalysts was based on the ISO 22197-1:2016 standard with some major modifications. With regard to the real environmental application, compared to the standard pollutant concentration of 1.0 ppmv, a lower concentration of 0.1 ppmv was used. A variety of slit height (ranged from 5 mm to 25 mm) and the rate of volume flow (ranged from 1.5 to 11.0 L min^{-1}) were performed, thus, the flow conditions were different from those given in the ISO standard. The data were evaluated using different ways, as it described below in detail.

The experimental set-up consisted of a gas supply part, the photoreactor, and a chemiluminescent Horiba APNA 370 NO-NO$_x$ gas analyser (SFig. 2). The reaction mixture was prepared by mixing dry and wet air with NO/N$_2$ or NO$_2$/N$_2$ (both 49.9 ppmv; Messer Technogas, Ltd., Czech Republic) streams to obtain a required concentration of 0.1 or 1.0 ppmv at air relative humidity of 50%. Differently from the ISO standard, the set-up was equipped with twelve Bronkhorst flow regulators (Bronkhorst High-Tech B.V., Ruurlo, Netherlands) enabling to prepare with high accuracy gas streams in a wide range of rate of volume flow at 0.1 or 1.0 ppmv NO or NO$_2$ concentrations. The samples on glass substrate were irradiated with black-light fluorescence lamps (Philips BLB 15 W, a length of 45 cm) in a planar arrangement, emitting dominant wavelength of 365 nm. Irradiation intensity of precisely 1.0 mW cm^{-2} was achieved by an appropriate distance between samples and lamps. The irradiation of samples caused no temperature changes in this experimental set-up.

Photocatalytic testing was performed using the reactor recommended by ISO 22197-1:2016, made of chemically inert polytetrafluorethylene to prevent the adsorption of pollutants and withstand irradiation of near-UV light. The dimensions of the reactor are 32 cm in length and 5 cm in width. Height-adjustment plates of different thicknesses provided a suitable placement of samples for the gas stream to pass exclusively through the space (here termed as a slit height) between the sample surface and the optical window. According to ISO standard, the slit height of 5 mm ± 0.5 mm corresponds to the reactor volume of 80 cm^3. The standard rate of volume flow of 3000 cm^3 min^{-1} corresponds to the air flow velocity of 0.2 m s^{-1}. The use of height-adjustment plates of different thicknesses significantly affected the other parameters, i.e., the reactor volume, velocity, space time and space velocity, for a given ranges of the rates of volume flow. For instance, the highest air flow in the reactor was 11000 cm^3 min^{-1} compared to lowest one of 1500 cm^3 min^{-1}. This approach enabled to perform the photocatalytic experiments at a wide range of flow conditions (Table 1). All photocatalytic experiments were performed in triplicate for the verification of the stability and repeatability with the data variation less than 10%.

2.3. Photocatalytic parameters and their definition

As the study is aimed at achieving the decrease in the total concentration of nitrogen oxides, the results are expressed using the concentration of composite NO$_x$ species, which include a sum of NO and NO$_2$. The quantification of the NO$_x$ concentration variation due to the photocatalytic process was performed in two ways.

Firstly, the NO$_x$conversion/% was calculated as a difference in the NO$_x$ concentration in the gas stream at the reactor inlet and at the reactor outlet related to the NO$_x$ inlet concentration

$$\mathrm{NO}_x conversion/\% = \frac{c_{in} - c_{out}}{c_{in}} \times 100$$

where c_{in} is the inlet concentration of NO$_x$, c_{out} is the outcome concentration of NO$_x$. Hereby, defined conversion is a directly measurable quantity suitable for the independent determination of the variation of the reaction rate with the flow parameters.

Secondly, the NO$_x$reaction rate/μmol m^{-2} h^{-1}, here denoted as -r (NO$_x$), expressed the rate of the decrease in the NO$_x$ concentration in unit time on a unit irradiated area, was calculated at the beginning of the test and after achieving the steady-state

$$-r(\mathrm{NO}_x) = (\varDelta \mathrm{NO} \ or \ \varDelta \mathrm{NO}_2) - (\varDelta \mathrm{NO}_x)$$

where $\varDelta$NO or $\varDelta$NO$_2$ is the difference between the concentration at the beginning of the test and after achieving the steady-state of NO or NO$_2$ and $\varDelta$NO$_x$ is the difference between the concentration at the beginning of the test and after achieving the steady-state of NO$_x$. Note that the reaction rate itself is already a dependent quantity because the rate of volume flow and input pollutant concentration are included in the calculation. Consequently, with increasing the rate of volume flow the reaction rate increases, even if the conversion itself decreases. Therefore, the interpretation of the

Table 1

An overview of process parameters of the photocatalytic experiments performed with photocatalytic layer of 50 cm^2.

Slit height mm	Reactor volume/ cm^3	Volume per irradiated area/ cm^3 cm^{-2}	Volume rate of flow/ cm^3 min^{-1}	Air flow velocity/ m s^{-1}	Space time/ min	Space velocity/ min^{-1}
5	80	1.6	1500	0.10	0.05	19
			3000	0.20	0.03	38
			5000	0.33	0.02	63
			7000	0.47	0.01	87
			9000	0.60	0.01	113
			11000	0.73	0.01	138
10	160	3.2	1500	0.05	0.11	9
			3000	0.10	0.05	19
			5000	0.17	0.03	31
			7000	0.23	0.02	44
			9000	0.30	0.02	56
			11000	0.36	0.02	69
20	320	6.4	1500	0.03	0.21	5
			3000	0.05	0.11	9
			5000	0.08	0.06	16
			7000	0.12	0.05	22
			9000	0.15	0.04	29
			11000	0.18	0.03	34
25	400	8.0	1500	0.02	0.27	4
			3000	0.04	0.13	8
			5000	0.07	0.08	13
			7000	0.09	0.06	18
			9000	0.12	0.04	23
			11000	0.15	0.04	28

rate of volume flow dependent data should be based on precisely defined quantities. In the following the presentation and discussion of the experiment outcomes were primarily based on the NO$_x$ conversion data, however, for comparison purposes also selected reaction rate data are included. Used notation of NO$_x$ reaction rate "-r (NO$_x$)" may be referred to in the literature as de(NO$_x$) (Zouzelka and Rathousky, 2017; Mills et al., 2020).

The NO$_x$ concentration changes due to the photocatalytic degradation were studied depending on three parameters, i.e., the slit height, volume rate of flow and velocity. The ranges of slit height (5–25 mm) and rate of volume flow (1.5–11.0 L min^{-1}) were independent parameters varied in the experiments in the given ranges. On the other hand, velocity (in unit of m s^{-1}) is a complex variable because its values are affected by the slit height. As with increasing the slit height also the reactor volume increased, the lower values of velocity were achieved at the same rate of volume flow. Consequently, the ranges of velocities were different for different slit heights.

The space time (or the retention time; min) was calculated as a reciprocal of the space velocity divided by the volume rate of flow and the reactor volume.

In addition, the uptake coefficients γ (dimensionless quantity) and the surface deposition velocity $v_{surf.}$ (m s^{-1}) were calculated, to take into an account the reactor geometry (El Zein and Bedjanian, 2012; Ifang et al., 2014) . Moreover, these quantities enable to compare quantitatively the performance characteristics determined using different experimental set-ups.

In STable 1 and 2 the results of the photocatalytic degradation of NO and NO$_2$ under different experimental conditions are summarized. In the following text, to clearly present the experimental data major trends and dependencies were discussed, focused in particular on FN2 material and the lower pollutant concentration (0.1 ppmv) as the representation of the real concentration in the environment. Higher concentration of pollutants (1.0 ppmv) and P25 material were then included into the discussion for the comparison purpose.

3. Results

3.1. Morphological and structure properties of photocatalytic layers

The obtained X-ray diffraction data (Fig. 1a) show that P25 coating is mainly consists of anatase (88%) and rutile (12%), while in the FN2 coating the presence of a binder was revealed. The most abundant phase was again anatase (75%) and rutile (10%), in addition the inorganic binder (13%), was observed. Almost 2% of the total content was an unidentified phase, probably the residues of the binder.

Both anatase and rutile possess a tetragonal structure. Anatase exhibited the diffraction peaks indexed at (101) 29.57°, (103) 43.27°, (004) 44.37°, (112) 45.27°, (200) 56.47°, (105) 64.05° and (211) 65.18°. Rutile diffraction peaks are indexed
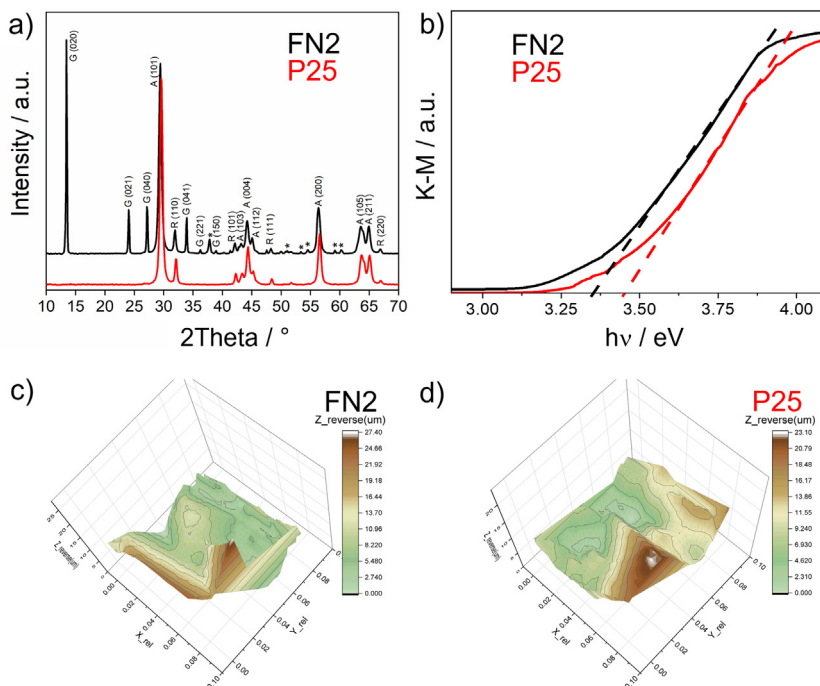
Fig. 1. (a) XRD patterns of P25 (red) and FN2 coating (black). The diffraction line corresponding to rutile (R), anatase (A) and binder (G) with significant diffractions are marked. Not identified maxima are marked by *. (b) UV–Vis diffuse reflectance spectra. (c) and (d) Topography of FN2 (c) and P25 (d) coatings, respectively, determined by nanoindentation mapping. K–M, the Kubelka–Munk function. (For interpretation of the references to colour in this figure legend, the reader is referred to the web version of this article.)

at position of (110) 32.07°, (101) 42.27°, (111) 48.37° and (220) 66.87°. Other diffraction peaks on the FN2 diffractogram correspond to the sulphate binder ((020) 13.45°, (021) 24.05°, (040) 27.15°, (041) 33.95°, (221) 36.25° and (150) 38.95°). Using the Rietveld refinement technique, the coherent mean particle size of 17 nm for anatase and 21 nm for rutile were also determined Rietveld (1969) and Cheary et al. (2004).

The diffuse reflectance spectra of the FN2 and P25 coatings exhibited an absorption edge below 400 nm due to the band gap absorption of the TiO_2 P25 nanoparticles (Fig. 1b). The absorption energy edges were 3.40 and 3.28 eV for P25 and FN2, respectively. The observed red shift in the absorbance spectrum of FN2 seems to be due to the interactions between the inorganic binder and TiO_2 nanoparticles.

Nanoindentation mapping (Figs. 1c and 1d) shows the surface of both FN2 and P25 coatings is highly irregular, with substantial protrusions and depressions on the surface, ranging from units to tens of micrometres.

HRTEM images (SFig. 3) confirmed the well crystalline anatase structure in both P25 and FN2 materials, well resolved (101) lattice fringes with distance of 0.35 nm being observed. These results were consistent with the XRD analysis, where particularly a strong (101) reflection of anatase was identified. The HRTEM image of FN2 shows also the presence of an inorganic binder and distinctly porous structure of this material. The SEM images (SFig. 4) show the highly porous and rough morphology of P25 and to a lesser degree of FN2. The surface roughness of both materials is expected to influence the flow type regime and to contribute to the formation of vortexes, and, thus, enhance in the degree of mixing. The thickness of the photocatalytic layers of both studied materials was 2 μm.

The comparison of the adsorption isotherms of nitrogen at ca 77 K on the FN2 and P25 coatings (not shown here) showed that the FN2 coating demonstrated a larger Brunauer–Emmett–Teller (BET) surface area (82 m^2 g^{-1}) compared to the P25 (47 m^2 g^{-1}). The binder presence probably led to the creation of a more developed porous texture. Concerning the porosity, the adsorption isotherms indicate the presence of very wide mesopores or macropores, whose width exceeded 30 nm (Table 2).

3.2. Photocatalytic abatement of NO

The effect of the slit height

The effect of the slit height showed that NO_x conversion differed considerably (Fig. 2). For both P25 and FN2, significant NO_x conversions of 60%–80% were observed for the lower rate of volume flow (1.5 and 3.0 L min^{-1}) and the lowest slit height (5 and 10 mm) (Fig. 2 a, b). The NO_x conversion decreased with increasing of rate of volume flow and with the
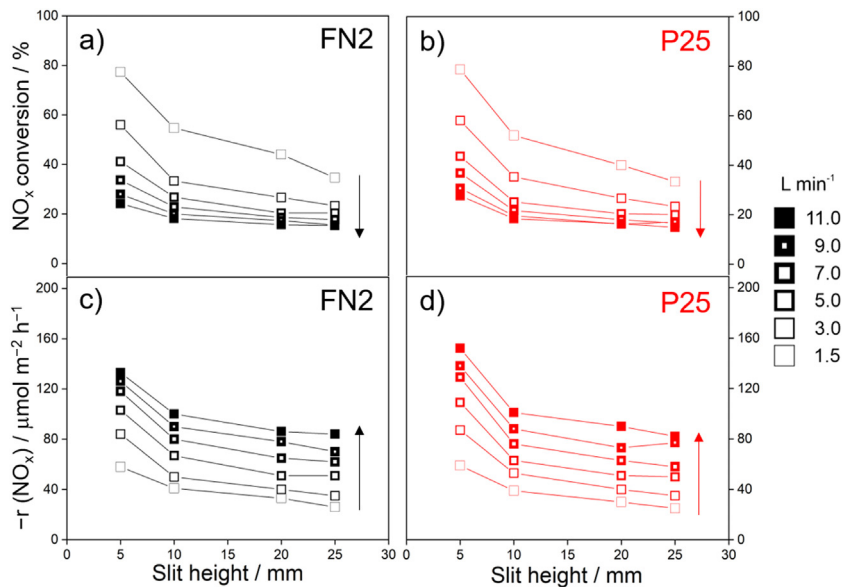
Fig. 2. The plot of the variation in the NO_x conversion and reaction rate with the slit height for inlet concentration of 0.1 ppmv NO for FN2 (a) and (c) and for P25 (b) and (d). The rate of volume flow is the parameter of the curves.

Table 2
Structural and morphological properties of photocatalytic coatings.

Photocatalyst	XRD[a] / %	XRD[a] / nm	BET[b] / nm	S_{BET}[b] / m^2 g^{-1}
	Anatase/Rutile/Binder	Anatase/Rutile/Binder		
FN2	77/10/13	16/22/133	nd	82
P25	88/12/0	16/22/0	28	47

[a]crystallite weight/% and size/nm determined by X-ray diffraction.
[b]particles size/nm and specific surface area/m^2 g^{-1} calculated from nitrogen adsorption isotherms.

increasing slit height. Interestingly, while with increasing rate of volume flow the NO_x conversions approached to each other. Thus, for the rate of volume flow of 5.0–11.0 L min^{-1} and the slits ranged from 5 to 25 mm in width, the conversion was roughly constant (20%).

For the inlet NO concentration of 1.0 ppmv, the NO_x conversions were significantly lower than for 0.1 ppmv — a decrease from 80% to 35% (FN2) and 16% (P25) (SFig. 5). Similarly, the highest NO_x conversions were observed using the lowest rate of volume flow (1.5 and 3.0 L min^{-1}) and slit height (5 mm). For the rate of volume flow from 5.0 to 11.0 L min^{-1} practically neither the influence of the slit height nor of the rate of volume flow was found. For the reaction rate similar trends were obtained. However, in the addition to the rate of volume flow, the reaction rate calculations also depend on the inlet NO concentration, resulting in much higher reaction rates compared to the experiments with the inlet concentration of 0.1 ppmv.

Concerning the reaction rate, completely opposite trend can be seen (Fig. 2b, d). This was due to the effect of the different rate of volume flow included in the calculation of the reaction rate. Consequently, the highest reaction rates were achieved for the highest rate of volume flow. The reaction rates gradually decreased with increasing slit height, following the same trend as for the NO_x conversion. The highest NO_x removal (ca. 130 μmol m^{-2} h^{-1}) was obtained using the rate of volume flow of 7.0–11.0 L min^{-1} and the lowest slit height, the lowest reaction rate being for lower flows with higher slits (ca. 30 μmol m^{-2} h^{-1}).

The effect of the rate of volume flow

Generally, the NO_x conversion values decreased gradually with increasing rate of volume flow for all the slit heights (Fig. 3a). The most significant variations in the NO_x conversion were observed for the lowest both rates of volume flow and slit heights. For the highest rates of volume flow in range of 9.0–11.0 L min^{-1} and the slit heights from 10 to 25 mm, there was practically no effect of these parameters.

As the rate of volume flow increased, the reaction rate of NO_x degradation increased as well (Fig. 3b). The reaction rate was significantly higher for the 5 mm slit height. For P25, the same trend was observed and also the reaction rates of NO_x degradation were comparable.
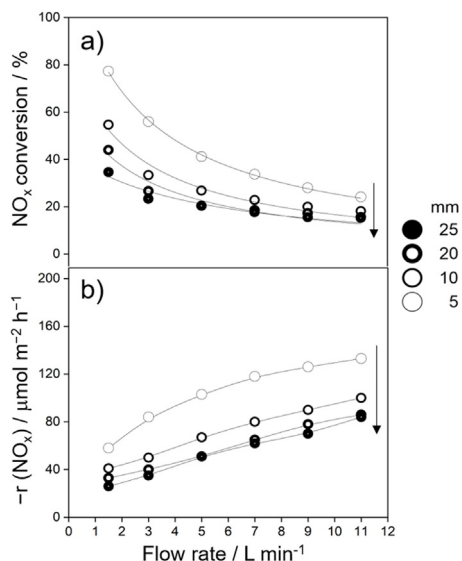
Fig. 3. Variation in the NO_x conversion (a) and reaction rate (b) with the rate of volume flow for the FN2 material, the slit height being the parameter. The inlet NO concentration of 0.1 ppmv.
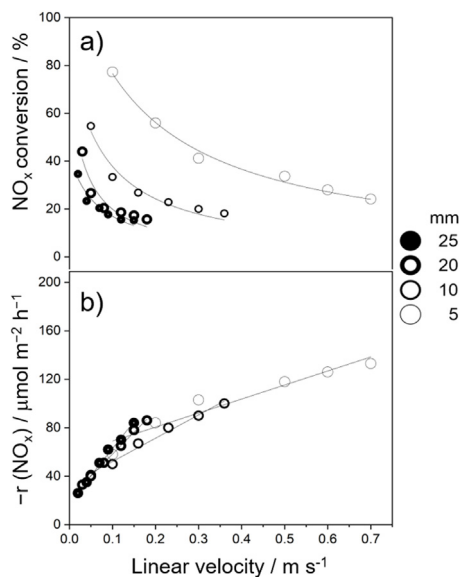

Fig. 4. Variation in the NO_x conversion (a) and reaction rate (b) on FN2 with the velocity of the flowing air, the slit height being the parameter. The inlet NO concentration of 0.1 ppmv.

The effect of the air flow velocity

The dependence of the NO_x conversion or reaction rate on the velocity is expressed, which is a parameter suitable for the comparison of the real wind condition in the environment (Fig. 4). However, it is a complex variable as explained earlier in Section 2.3.

As the trends for P25 and FN2 were comparable, we focused on the discussing the results for FN2. In general, Fig. 4a shows that with increasing air flow velocity the NO_x conversion decreased. The highest NO_x conversions throughout the whole range of velocities included were observed for the slit 5 mm in height, where the photoreactor volume was the smallest (80 cm^3). Such small reactor volume enabled to achieve a wide range of velocities from 0.1 to 0.7 m s^{-1}, which are often encountered in real applications. The space time corresponding to the highest velocity equals only 0.436 s, which is much shorter compared to number of published papers, but relevant for real applications.
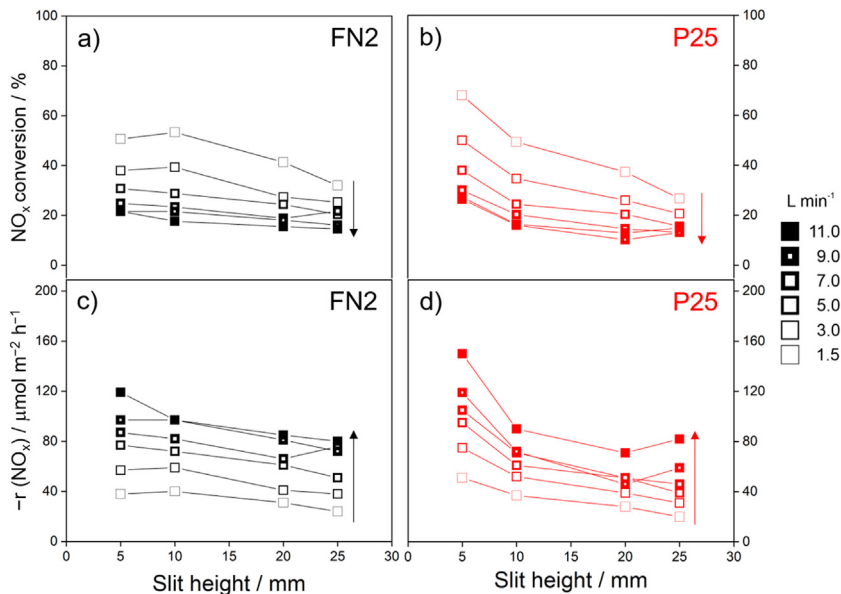
Fig. 5. Variation in the NO_x conversion and reaction rate with the slit height for inlet concentration of 0.1 ppmv NO_2 for FN2 (a) and (c) and for P25 (b) and (d). The rate of volume flow is the parameter of the curves.

With increasing the slit height, the reactor volume increased resulting in narrowing the range of velocities achieved. It is obvious that for higher slits (10–25 mm), the conversions decreased rapidly and step by step coming closer to each other (Fig. 4a). However, even the system with the highest slit (25 mm, representing the largest reactor volume of 400 cm^3) was able to degrade reasonable amounts of NO (ca. 15%). Consequently, the effect of the slit height was seemed to be not a critical factor.

For the higher NO inlet concentration of 1.0 ppmv NO, the general trends were similar, but a significantly lower NO_x conversion in comparison with the experiments at 0.1 ppmv NO was observed and also the differences between FN2 and P25 were more evident. The initial NO_x conversion is 35% for FN2 and 18% for P25, compared to 80% of conversion for 0.1 ppmv NO for both materials.

The reaction rate was directly proportional to the velocity, the slit height having only minor effect. This type of plots seems convenient for the assessment of the efficiency of the photocatalytic technology as it directly shows the variation of the reaction rate on velocity, which is the very parameter known from the standard hydrometeorological measurements.

3.3. Photocatalytic abatement of NO_2

The effect of the slit height

Interestingly, for FN2, compared to the experiments with NO 0.1 ppmv (Fig. 2), the effect of the slit height was almost negligible (Fig. 5). This observation was reflected in the values of the reaction rates and NO_x conversion of NO_2 degradation, which were for FN2 comparable for all slit heights. The effect of the rate of volume flow was much pronounced, the NO_x conversion and reaction rate decreasing with increasing rate of volume flow.

On the other hand, for P25, a comparable trend in NO_x conversion and reaction rates was observed for the same NO and NO_2 concentration of 0.1 ppmv. The effects of both the slit height and rate of volume flow on the conversion were more marked than for FN2, especially for the slit height of 5 mm and the rate of volume flow of 1.5 L min^{-1} (Fig. 5b). The reaction rate and NO_x conversion gradually decreased with increasing slit height and rate of volume flow and a limiting value as for FN2 were not achieved.

Generally, in comparison with the NO abatement, a slightly lower amount of converted NO_2 and its lower reaction rates were observed at otherwise identical conditions. This observation is in an agreement with Ifang et al. (2014), who suggested the gas-phase photolysis of NO_2 as a suitable explanation. Also a competition between O_2 and NO_2 for scavenging the electrons at the photocatalyst surface and NO_2 disproportionation, which lead to the NO_2 reduction instead to its required oxidation, may support this conclusion (Monge et al., 2010). However, as the data obtained show, this difference is not decisive obstacle for the successful application of these coatings.

For the inlet concentration of 1.0 ppmv NO_2, the situation was very similar to the degradation of 1.0 ppmv NO in terms of observed trends. Moreover, a major decrease in the absolute values of the NO_x conversion in comparison with the lower inlet concentration of 0.1 ppmv NO_2 was observed.

The effect of the rate of volume flow

It is obvious that the effect of the variation in rate of volume flow was much more pronounced than that of the slit height (SFig. 6). Compared to the experiments with 0.1 ppmv NO (Fig. 3), the beneficial effect of the smallest slit height (5 mm) and the slowest rate of volume flow (1.5 L min^{-1}) was significantly smaller. The data for NO$_2$ also show that even if the conversion gradually decreased with the rate of volume flow, the system was able to degrade sizeable concentrations of NO$_2$, even at the highest rate of volume flow (11.0 L min^{-1}) and all slit heights included.

For the experiments with 1.0 ppmv NO$_2$, the NO$_x$ conversion decreased significantly for the lower rates of volume flow of 1.5 to 3.0 L min^{-1}. For higher rates of volume flow, the NO$_x$ conversion was not much influenced by the slit height and rate of volume flow. Probably, a stationary state was achieved, where the NO$_x$ conversion did not depend on the flow conditions performed.

The effect of the air flow velocity

In general, the observed trends were similar to the corresponding data obtained with 0.1 ppmv NO (SFig. 7). The differences are in the total NO$_x$ conversion, which was higher for the NO degradation. The differences due to the slit height were more marked for the lowest velocities, while with their increase the effect of the slit height was only minor. For P25, the trends were comparable with the system of degradation 0.1 ppmv NO.

In experiments with the inlet concentration of 1 ppmv NO$_2$, the conversion was significantly lower (40% for FN2 and 12% for P25) in comparison with 0.1 ppmv NO$_2$ (65% and 70%, respectively) and the differences between FN2 and P25 were more pronounced. With increasing the velocity, the NO$_x$ conversion decreased, but at higher velocities, given the slit height for individual systems, the amount of converted NO$_x$ was already comparable.

4. Discussion

Relatively subordinate effect of the slit height indicates there was substantial degree of mixing in a direction perpendicular to the flow direction. Therefore, the flow should not be described as a laminar one, which is characterized by a parabolic velocity profile and the exclusive transport of molecules in the perpendicular direction by molecular diffusion. Even if the Reynold's number (*Re*) corresponding to the velocity calculated from the volume rate of flow and the cross-sectional area of the reactor was as low as 50 or 200, this is not a proof that the flow was really laminar. Problematic is also the way how to calculate the length scale ("effective diameter") inserted into the formula for *Re* for a slit shaped channel (Demeestere et al., 2004; El Zein and Bedjanian, 2012; Ifang et al., 2014; Mothes et al., 2018; Uruba, 2019).

The comparison with other published studies showed there are both similarities and differences. For instance, Ballari and co-workers (2010) observed the slit height did not have any effect on the conversion of NO$_x$ (Ballari et al., 2010, 2011), which is in an agreement with the present study. The range of slit heights was rather narrow, only 2–4 mm. However, the authors described the flow as a laminar one with a fully developed parabolic velocity profile with entrance effect only within the first 10% of the slit length. In another study, De Melo and Trichês (2012) reported that with the increasing rate of volume flow, the degradation rate and conversion of NO$_x$ increased and decreased, respectively. These observations are in an agreement with the present study, even if achieved at markedly different experimental conditions, such as very low velocity of the flowing air.

Moreover, the construction and geometry of the reactor itself plays very important role in the determined efficiency of the photocatalytic process due to their significant effect on the flow regime inside the reactor. Several authors reported that different suitable reactor design eliminating the diffusion limitations (Tomašić et al., 2008; Hüsken et al., 2009; Hunger et al., 2010; Ifang et al., 2014; Mothes et al., 2018; Ballari et al., 2020, 2011; de O.B. Lira et al., 2019; Lira et al., 2020; Oliveira De Brito Lira et al., 2021).

Very important role in the development of the character of the air flow along the photocatalyst coating plays its roughness. Both SEM and nanoindentation mapping (Fig. 1c, d and SFig. 4) confirm the irregularities of the surface in the range up to ca. 30 µm. It can be expected that these irregularities protrude across the laminar sublayer, which may lead to the tearing off the boundary layer. Therefore, a transport is not limited to the diffusion of single molecules, but it is substantially enhanced by larger aggregates due to vortexes formed.

Fig. 6 shows a comparison of uptake coefficients for the FN2 and the inlet concentration of NO or NO$_2$ of 0.1 ppmv. There are several interesting conclusions, which can be drawn from this comparison. First, the performance towards NO$_2$ is only slightly lower than for NO. Second, the effect of the slit height is practically negligible. Finally, the uptake coefficient is decisively determined by the rate of volume flow, equalling about 2×10^{-4} and 10×10^{-4} for 1.5 and 11.0 L min^{-1}, respectively.

Fig. 7 shows an interesting comparison of the NO$_x$ conversion for FN2 and P25 for the inlet concentration of 0.1 ppmv NO or NO$_2$. Only the limit parameters were selected, i.e., the lowest (5 mm) and highest (25 mm) slit height and the lowest (1.5 L min^{-1}) and highest
(11.0 L min^{-1}) rate of volume flow. The performance of both photocatalysts (FN2 and P25) was comparable, the differences were only minor. With the exception of the limiting lowest slit height and rate of volume flow, there is not much difference between the performance towards both pollutants.

Besides the convective dispersion in the direction perpendicular to the flow there is also the question whether there is some marked axial dispersion. According to the published data, the dispersion coefficient should be very low for the conditions of the experiments according to the ISO standard (ISO 22197-1:2016). However, the correlations presented by Levenspiel (1999) in his famous book provided a different image. Actually, there should be some degree of mixing in the axial direction.
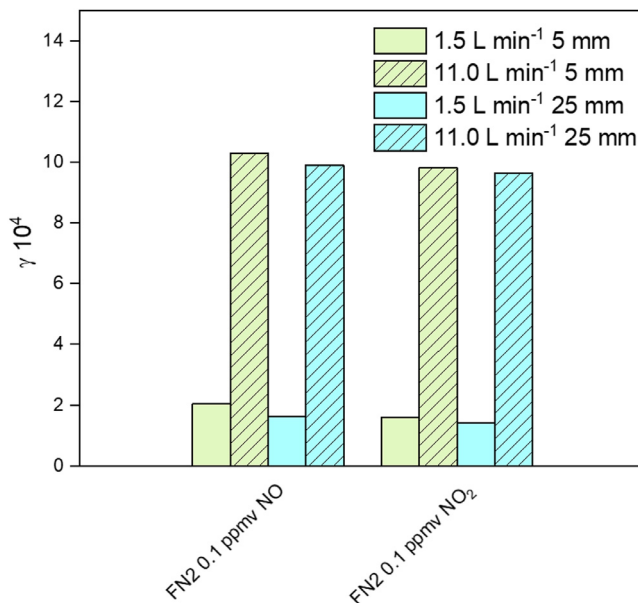
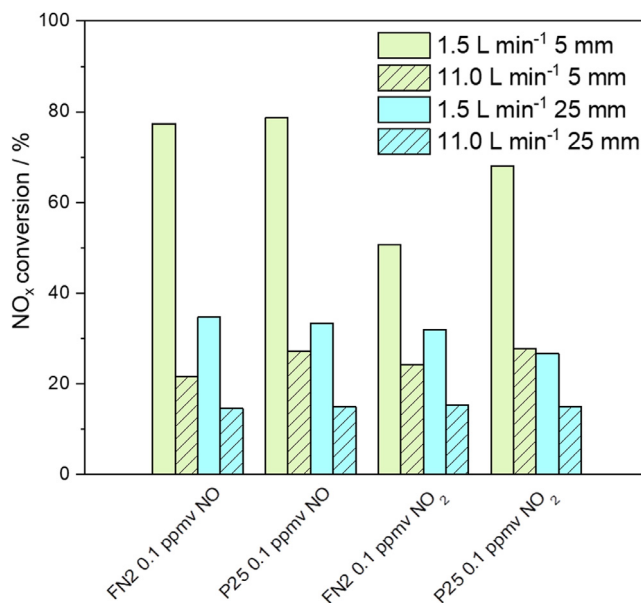**Fig. 6.** Uptake coefficient summary for the FN2 coating.

Fig. 7. Comparison of the photocatalytic performance of FN2 and P25 coatings at the rates of volume flow and slit heights representing their limits.

5. Conclusions

In the study, we investigated the ability of two commercial photocatalysts, Aeroxide$^{\circledR}$ TiO$_2$ P25 (Evonik Industries, Germany) and FN NANO$^{\circledR}$ 2 (Advanced Materials-JTJ, Czech Republic).

The degradation of NO and NO$_2$ (0.1 and 1.0 ppmv) under high air flow velocities was studied. At these velocities, the photocatalytic efficiency was determined for various slit heights (5–25 mm) and rates of volume flow (1.5–11.0 L min^{-1}). Both photocatalysts achieved substantial NO and NO$_2$ abatement. Slit height had a negligible effect, indicating that there was a substantial degree of mixing in the direction perpendicular to the flow, which is supported by nanoindentation technique showing that the surface roughness contributed to the formation of vortexes and enhancement of the mass transport. The extensive data obtained show that the coatings of the industrially produced FN2 photocatalytic material containing inorganic binder exhibited substantial photocatalytic performance, even at rather demanding flow conditions,

such as higher slits (up to 5 times compared to the ISO standard) and substantially increased rates of volume flow (up to 4 times with respect to the standard mentioned). As the values of the reaction uptake were in the range 10^{-4}–10^{-3} showing the performance of this commercial coating at realistic environmental conditions (regarding the pollutant concentration and the rate of volume flow) appear to be excellent. Moreover, its performance towards NO_2 is only slightly lower than that towards NO. This is of major importance as both pollutants are present in the polluted air at different ratio, which may vary within a day or season of the year.

CRediT authorship contribution statement

Eliska Mikyskova: Conceptualization, Methodology, Investigation, Writing – original draft. **Ivana Martiniakova:** Investigation, Data curation. **Radek Zouzelka:** Writing – review & editing. **Jiri Rathousky:** Conceptualization, Funding acquisition, Project administration, Supervision.

Declaration of competing interest

The authors declare that they have no known competing financial interests or personal relationships that could have appeared to influence the work reported in this paper.

Acknowledgements

Appendix A. Supplementary data

Supplementary material related to this article can be found online at https://doi.org/10.1016/j.eti.2022.102820.

References

Ao, C.H., Lee, S.C., 2003. Enhancement effect of TiO_2 immobilized on activated carbon filter for the photodegradation of pollutants at typical indoor air level. Appl. Catal. B Environ. 44, 191–205. http://dx.doi.org/10.1016/S0926-3373(03)00054-7.

Ballari, M.M., Hunger, M., Hüsken, G., Brouwers, H.J.H., 2010. Modelling and Experimental Study of the NO_x Photocatalytic Degradation Employing Concrete Pavement with Titanium Dioxide. vol. 151, pp. 71–76. http://dx.doi.org/10.1016/j.cattod.2010.03.042.

Ballari, M.D.L.M., Satuf, M.L., Alfano, O.M., 2020. Photocatalytic reactor modeling: application to advanced oxidation processes for chemical pollution abatement. Heterog. Photocatal. 265–301. http://dx.doi.org/10.1007/978-3-030-49492-6_8.

Ballari, M.M., Yu, Q.L., Brouwers, H.J.H., 2011. Experimental Study of the NO and NO_2 Degradation by Photocatalytically Active Concrete. vol. 161, pp. 175–180. http://dx.doi.org/10.1016/j.cattod.2010.09.028.

Binas, V., Venieri, D., Kotzias, D., Kiriakidis, G., 2017. Modified TiO_2 based photocatalysts for improved air and health quality. J. Mater. 3, 3–16. http://dx.doi.org/10.1016/j.jmat.2016.11.002.

Boyjoo, Y., Sun, H., Liu, J., Pareek, V.K., Wang, S., 2017. A review on photocatalysis for air treatment: From catalyst development to reactor design. Chem. Eng. J. 310, 537–559. http://dx.doi.org/10.1016/j.cej.2016.06.090.

Castrillón, S.R.V., De Lasa, H.I., 2007. Performance evaluation of photocatalytic reactors for air purification using Computational Fluid Dynamics (CFD). Ind. Eng. Chem. Res. 46, 5867–5880. http://dx.doi.org/10.1021/ie060696q.

Cheary, R.W., Coelho, A.A., Cline, J.P., 2004. Fundamental parameters line profile fitting in laboratory diffractometers. J. Res. Natl. Inst. Stand. Technol. 109, 1–25. http://dx.doi.org/10.6028/jres.109.002.

Chen, M., Chu, J.-W., 2011. NO_x photocatalytic degradation on active concrete road surface — From experiment to real-scale application. J. Clean. Prod 19, 1266–1272. http://dx.doi.org/10.1016/j.jclepro.2011.03.001.

Cordero, J.M., Hingorani, R., Jimenez-relinque, E., Grande, M., Borge, R., Narros, A., Castellote, M., 2020. Science of the Total Environment NO_x removal ef fi ciency of urban photocatalytic pavements at pilot scale. Sci. Total Environ. 719, 137459. http://dx.doi.org/10.1016/j.scitotenv.2020.137459.

De Melo, J.V.S., Trichês, G., 2012. Evaluation of the Influence of Environmental Conditions on the Efficiency of Photocatalytic Coatings in the Degradation of Nitrogen Oxides (NO_x). vol. 49, http://dx.doi.org/10.1016/j.buildenv.2011.09.016.

Demeestere, K., Visscher, A. De, Dewulf, J., Leeuwen, M. Van, Langenhove, H. Van, 2004. A new kinetic model for titanium dioxide mediated heterogeneous photocatalytic degradation of trichloroethylene in gas-phase. Appl. Catal. B Environ. 54, 261–274. http://dx.doi.org/10.1016/j.apcatb.2004.06.020.

Devahasdin, S., Fan, C., Li, K., Chen, D.H., 2003. TiO_2 photocatalytic oxidation of nitric oxide: Transient behavior and reaction kinetics. J. Photochem. Photobiol. A 156, 161–170. http://dx.doi.org/10.1016/S1010-6030(03)00005-4.

Dillert, R., Stötzner, J., Engel, A., Bahnemann, D.W., 2012. Influence of inlet concentration and light intensity on the photocatalytic oxidation of nitrogen (II) oxide at the surface of aeroxide$^{®}$ TiO_2 P25. J. Hazard. Mater. 211–212, 240–246. http://dx.doi.org/10.1016/j.jhazmat.2011.11.041.

El Zein, A., Bedjanian, Y., 2012. Interaction of NO_2 with TiO_2 surface under UV irradiation: Measurements of the uptake coefficient. Atmos. Chem. Phys. 12, 1013–1020. http://dx.doi.org/10.5194/acp-12-1013-2012.

Guerreiro, C.B.B., Foltescu, V., Leeuw, F.de., 2014. Air quality status and trends in Europe. Atmos. Environ. 98, 376–384. http://dx.doi.org/10.1016/j.atmosenv.2014.09.017.

Guo, Q., Zhou, C., Ma, Z., Yang, X., 2019. Fundamentals of TiO_2 photocatalysis: Concepts, mechanisms, and challenges. Adv. Mater. 31, 1–26. http://dx.doi.org/10.1002/adma.201901997.

Hunger, M., Hüsken, G., Brouwers, H.J.H., 2010. Photocatalytic degradation of air pollutants — From modeling to large scale application. Cem. Concr. Res. 40, 313–320. http://dx.doi.org/10.1016/j.cemconres.2009.09.013.

Hüsken, G., Hunger, M., Brouwers, H.J.H., 2009. Experimental study of photocatalytic concrete products for air purification. Build. Environ. 44, 2463–2474. http://dx.doi.org/10.1016/j.buildenv.2009.04.010.

Ifang, S., Gallus, M., Liedtke, S., Kurtenbach, R., Wiesen, P., Kleffmann, J., 2014. Standardization methods for testing photo-catalytic air remediation materials: Problems and solution. Atmos. Environ. 91, 154–161. http://dx.doi.org/10.1016/j.atmosenv.2014.04.001.

Imoberdorf, G.E., Irazoqui, H.A., Alfano, O.M., Cassano, A.E., 2007. Scaling-up from first principles of a photocatalytic reactor for air pollution remediation. Chem. Eng. Sci. 62, 793–804. http://dx.doi.org/10.1016/j.ces.2006.10.004.

Levenspiel, Octave, 1999. Chemical Reaction Engineering. John Wiley & Sons, New York.

Lira, J.O.B., Riella, H.G., Padoin, N., Soares, C., 2020. CFD + DoE optimization of a flat plate photocatalytic reactor applied to NO_x abatement. Chem. Eng. Process. 154, 107998. http://dx.doi.org/10.1016/j.cep.2020.107998.

Mills, A., Andrews, R., Han, R., O'Rourke, C., Hodgen, S., 2020. Supersensitive test of photocatalytic activity based on ISO 22197-1:2016 for the removal of NO. J. Photochem. Photobiol. A Chem. 400, 112734. http://dx.doi.org/10.1016/j.jphotochem.2020.112734.

Monge, M.E., George, C., D'Anna, B., Doussin, J.F., Jammoul, A., Wang, J., Eyglunent, G., Solignac, G., Daële, V., Mellouki, A., 2010. Ozone formation from illuminated titanium dioxide surfaces. J. Amer. Chem. Soc. 132, 8234–8235. http://dx.doi.org/10.1021/ja1018755.

Mothes, F., Ifang, S., Gallus, M., Golly, B., Boréave, A., Kurtenbach, R., Kleffmann, J., George, C., Herrmann, H., 2018. Bed flow photoreactor experiments to assess the photocatalytic nitrogen oxides abatement under simulated atmospheric conditions. Appl. Catal. B Environ. 231, 161–172. http://dx.doi.org/10.1016/j.apcatb.2018.03.010.

Muñoz, V., Casado, C., Suárez, S., Sánchez, B., Marugán, J., 2019. Photocatalytic NO_x removal : Rigorous kinetic modelling and ISO standard reactor simulation. Catal. Today 326, 82–93. http://dx.doi.org/10.1016/j.cattod.2018.09.001.

de O.B. Lira, J., Padoin, N., Vilar, V.J.P., Soares, C., 2019. Photocatalytic NO_x abatement: Mathematical modeling, CFD validation and reactor analysis. J. Hazard. Mater. 372, 145–153. http://dx.doi.org/10.1016/j.jhazmat.2018.07.009.

Oliveira De Brito Lira, J., Riella, H.G., Padoin, N., Soares, C., 2021. An overview of photoreactors and computational modeling for the intensification of photocatalytic processes in the gas-phase: State-of-art. J. Environ. Chem. Eng. 9, http://dx.doi.org/10.1016/j.jece.2021.105068.

Park, H., Park, Y., Kim, W., Choi, W., 2013. Surface modification of TiO_2 photocatalyst for environmental applications. J. Photochem. Photobiol. C Photochem. Rev. 15, 1–20. http://dx.doi.org/10.1016/j.jphotochemrev.2012.10.001.

Queffeulou, A., Geron, L., Archambeau, C., Le Gall, H., Marquaire, P.M., Zahraa, O., 2010. Kinetic study of acetaldehyde photocatalytic oxidation with a thin film of TiO_2 coated on stainless steel and CFD modeling approach. Ind. Eng. Chem. Res. 49, 6890–6897. http://dx.doi.org/10.1021/ie9017308.

Rietveld, H.M., 1969. A profile refinement method for nuclear and magnetic structures. J. Appl. Crystallogr. 2, 65–71. http://dx.doi.org/10.1107/s0021889869006558.

Talaiekhozani, A., Rezania, S., Kim, K., Sanaye, R., Mohammad, A., 2021. Recent advances in photocatalytic removal of organic and inorganic pollutants in air. J. Clean. Prod. 278, 123895. http://dx.doi.org/10.1016/j.jclepro.2020.123895.

Tomašić, V., Jović, F., Gomzi, Z., 2008. Photocatalytic oxidation of toluene in the gas phase: Modelling an annular photocatalytic reactor. Catal. Today 137, 350–356. http://dx.doi.org/10.1016/j.cattod.2008.05.017.

Uruba, V., 2019. Reynolds number in laminar flows and in turbulence. AIP Conf. Proc. 2118, http://dx.doi.org/10.1063/1.5114728.

Vogel, B., Vogel, H., Kleffmann, J., Kurtenbach, R., 2003. Measured and simulated vertical profiles of nitrous acid — Part II. Model simulations and indications for a photolytic source. Atmos. Environ. 37, 2957–2966. http://dx.doi.org/10.1016/S1352-2310(03)00243-7.

Wang, H., Wu, Z., Zhao, W., Guan, B., 2007. Photocatalytic oxidation of nitrogen oxides using TiO_2 loading on woven glass fabric. Chemosphere 66, 185–190. http://dx.doi.org/10.1016/j.chemosphere.2006.04.071.

Zouzelka, R., Rathousky, J., 2017. Photocatalytic abatement of NO_x pollutants in the air using commercial functional coating with porous morphology. Appl. Catal. B Environ. 217, 466–476. http://dx.doi.org/10.1016/j.apcatb.2017.06.009.